Journal of Orthopaedic Translation 51 (2025) 132–144

Contents lists available at ScienceDirect

Journal of Orthopaedic Translation

journal homepage: www.journals.elsevier.com/journal-of-orthopaedic-translation

Original article

JP4-039 protects chondrocytes from ferroptosis to attenuate osteoarthritis progression by promoting Pink1/Parkin-dependent mitophagy

Ya Xie [a,b,1], Zhongyang Lv [c,1], Weitong Li [a,b,1], JinTao Lin [c], Wei Sun [d], Hu Guo [b], Xiaoyu Jin [a,b], Yuan Liu [b], Ruiyang Jiang [e], Yuxiang Fei [b], Rui Wu [b], Dongquan Shi [a,b,e,f,g,*]

[a] Division of Sports Medicine and Adult Reconstructive Surgery, Department of Orthopedic Surgery, Nanjing Drum Tower Hospital Clinical College of Nanjing University of Chinese Medicine, 321 Zhongshan Road, Nanjing, 210008, Jiangsu, China
[b] Division of Sports Medicine and Adult Reconstructive Surgery, Department of Orthopedic Surgery, Nanjing Drum Tower Hospital, Affiliated Hospital of Medical School, Nanjing University, 321 Zhongshan Road, Nanjing, 210008, Jiangsu, China
[c] Department of Orthopedics, Nanjing Jinling Hospital, Affiliated Hospital of Medical School, Nanjing University, Nanjing, 210002, China
[d] Department of Orthopedic, The Jiangyin Clinical College of Xuzhou Medical University, Jiangyin, 214400, China
[e] Division of Sports Medicine and Adult Reconstructive Surgery, Department of Orthopedic Surgery, Nanjing Drum Tower Hospital, Clinical College of Xuzhou Medical University, Nanjing, 210008, Jiangsu, China
[f] State key laboratory of pharmaceutical biotechnology, Nanjing University, Nanjing, 210002, China
[g] Chemistry and Biomedicine Innovation Center, Nanjing University, Nanjing, 210002, China

ARTICLE INFO

Keywords:
Ferroptosis
JP4-039
Mitophagy
Osteoarthritis

ABSTRACT

Background: Osteoarthritis (OA) is the most common degenerative joint disease, and its main pathological mechanism is articular cartilage degeneration. The purpose of this study was to investigate the role of mitophagy in the pathogenesis of chondrocyte ferroptosis in OA.

Methods: The expressions of ferroptosis related proteins (GPX4, FTH1, COX2) and ubiquitin-dependent mitophagy related proteins (PARKIN, PINK1) in the intact and injured areas of OA cartilage were analyzed. Nitro oxide JP4-039, a mitochondrial targeting antioxidant, has bifunctional role of targeting mitochondria. Then we evaluated the potential protective effect of JP4-039 in OA using the destabilization of medial meniscus (DMM)-induced OA model, as well as tert-butyl hydrogen peroxide (TBHP)-treated primary mouse chondrocytes and human cartilage explants.

Results: The concentrations of iron and lipid peroxidation and the expression of ferroptosis drivers in the damaged areas of human OA cartilages were significantly higher than those in the intact cartilage. Pink1/Parkin-dependent mitophagy decreased in the injured area of human OA cartilage and was negatively correlated with ferroptosis. Then, the toxicity and effectiveness of JP4-039 are tested to determine its working concentration. Next, at the molecular biological level, we found that JP4-039 showed the effect of anti-chondrocyte ferroptosis. Moreover, it was verified on DMM-induced OA model mice, that JP4-039 could delay the progression of OA. Finally, JP4-039 was re-verified in vivo and in vitro to inhibit chondrocyte ferroptosis and delay the progression of OA by promoting Pink1/Parkin-dependent mitophagy.

Conclusion: JP4-039 inhibits ferroptosis of chondrocytes by promoting Pink1/Parkin-dependent mitophagy and delays OA progression.

1. Introduction

Osteoarthritis (OA) is the most common form of degenerative joint disorder and a leading cause of global disability [1,2]. OA is characterized by swelling and pain in the affected joints, and in severe cases, it may be accompanied by joint deformity, restricted movement, and ultimately lead to disability. The burden of disease caused by OA includes not only direct and indirect financial costs, but also individuals

* Corresponding author.Nanjing Drum Tower Hospital Clinical College of Nanjing University of Chinese Medicine, Nanjing, 210008, Jiangsu, China.
E-mail addresses: 459895571@qq.com (Y. Xie), zhongyanglv@163.com (Z. Lv), 1554845347@qq.com (W. Li), Jintao_lin@163.com (J. Lin), Sunw1988@outlook.com (W. Sun), 15050583626@163.com (H. Guo), 1152123889@qq.com (X. Jin), 952468149@qq.com (Y. Liu), jry1028@163.com (R. Jiang), 975778674@qq.com (Y. Fei), 18795950086@163.com (R. Wu), shidongquan@nju.edu.cn (D. Shi).
[1] These authors contributed equally to this work.

https://doi.org/10.1016/j.jot.2025.01.001
Received 8 July 2024; Received in revised form 5 December 2024; Accepted 2 January 2025

intangible living costs, including pain, fatigue, limited activity, reduced quality of life, and social limitations. Hence, with the incessant escalation of OA incidence, its associated burden is consistently mounting [3]. As societal and economic development continues, the escalating trends of obesity and aging are intensifying. The incidence of OA is projected to increase by approximately 50 % over the next 20 years, making it a significant public health challenge in the coming decades [4].

In the initial phase of our research, we classified osteoarthritis (OA) into four subtypes: the cartilage degradation-driven subtype, the bone remodeling-driven subtype, the pain-driven subtype, and the inflammation-driven subtype [5]. The principal pathological characteristics of OA manifest in the progressive degeneration and degradation of articular cartilage. Chondrocytes, the exclusive cell population within cartilage, assume a pivotal role, and the process of chondrocyte death plays a critically influential role in the progression of articular cartilage degeneration in OA. In recent years, various forms of chondrocyte death, including apoptosis, necroptosis, necrosis, autophagic cell death et al., have been demonstrated to be associated with the development of OA [6,7]. Different modes of cell death, either independently or in combination, collectively contribute to cartilage degeneration, thereby promoting the pathological progression of OA. The ferroptosis induced by iron-dependent lipid peroxidation has attracted considerable attention. This cellular death pathway exhibits significant differences at the genetic, morphological, and biological levels compared to previously identified programmed cell death [8]. Iron, an indispensable trace element, plays a pivotal role in human physiology. However, iron overload has been documented to elicit the accumulation of lipid reactive oxygen species (ROS), alterations in the expression of ferroptosis-associated proteins, and the demise of chondrocytes. This cascade of events ultimately results in heightened catabolism and reduced anabolism in chondrocytes [9,10]. Recent findings indicate that, within human osteoarthritis (OA), elevated concentrations of iron and lipid peroxidation, coupled with increased levels of ferroptosis drivers, are notably prevalent in the affected regions of articular cartilage compared to intact regions. Furthermore, through single-cell transcriptomics sequencing, a distinct subpopulation of chondrocytes exhibiting characteristic ferroptotic features was identified in the cartilage of individuals with OA. This revelation provides direct evidence of the involvement of chondrocyte ferroptosis in the pathological progression of OA [11].

As the epicenter of cellular energy metabolism, mitochondria serve as both the principal origin of intracellular reactive oxygen species (ROS) and the central hub for iron metabolism, playing a pivotal role in the maintenance of systemic iron homeostasis [12–14]. Prior investigations have demonstrated that, in the course of ferroptosis, mitochondria undergo morphological alterations characterized by a reduction in mitochondrial cristae and rupture of the outer mitochondrial membrane. These changes consequently result in impaired mitochondrial function [8,15–17]. Mitochondrial dysfunction, particularly stemming from dysregulated mitophagy, has been documented as a primary contributor, expediting the progression of OA [18–20]. Targeting the restoration of mitochondrial dysfunction is consequently regarded as a potentially efficacious therapeutic strategy for the disease.

The association between dysfunctional mitophagy and ferroptosis has been documented in the literature. However, a definitive investigation specifically addressing this relationship in the context of OA remains to be conducted [21]. Ferroptosis accompanies persistent chondrocyte demise attributed to mitochondrial dysfunction. Notably, lipophilic antioxidants and iron chelators have demonstrated efficacy in inhibiting ferroptosis. As a prospective intervention, we explored the use of JP4-039, a mitochondria-targeted nitroxide compound. This compound combines the free radical scavenger 4-hydroxy-2,2,6,6-tetramethylpiperidine-1-oxyl (TEMPO) with the mitochondria-targeting semigramicidin S peptide. The aim is to address and potentially mitigate the ongoing cellular damage associated with iron-induced cell death and the consequential impact on chondrocyte function [22]. And it has been proven that JP4-039 is an effective antioxidant [23]. Yet, the crucial question of whether JP4-039 can reinstate the mitophagy barrier to impede chondrocyte ferroptosis and consequently decelerate the progression of osteoarthritis (OA) remains unexplored and unreported. Hence, our proposed investigation aims to elucidate whether JP4-039 can effectively retard the progression of OA by preventing chondrocyte ferroptosis. Additionally, we intend to delve into the specific molecular mechanisms of JP4-039, exploring its potential to restore the pathway of mitophagy. This comprehensive study seeks to shed light on the intricate interplay between JP4-039, chondrocyte survival, and the modulation of mitophagy, providing valuable insights for potential therapeutic applications in OA.

2. Materials and methods

2.1. Ethics statement

Human articular cartilage and synovial fluid samples were acquired from knee osteoarthritis patients who underwent total knee arthroplasty, following approval from the Ethics Committee of Nanjing Drum Tower Hospital, Affiliated Hospital of Nanjing University School of Medicine (2020-156-01). Mouse experiments were conducted with full authorization and in compliance with the regulations of the Animal Care and Use Committee of Nanjing Drum Tower Hospital Clinical College, Nanjing University of Chinese Medicine (2020AE01102).

2.2. Clinical specimen collection

Human knee OA cartilage samples, obtained during knee arthroplasty at Nanjing Drum Tower Hospital, were categorized into intact (lateral condyles) and damaged (medial condyles) regions. Six pairs of cartilage samples were utilized to extract proteins for the measurement of indicators related to ferroptosis and mitophagy.

2.3. Animal study

Wild type C57BL/6 mice, were purchased from Model Animal Research Center of Nanjing University. All mice were kept under pathogen-free and 12 h light/dark cycle environment with free access to food and water. At 12 weeks of age, an osteoarthritis (OA) model was induced in male C57BL/6 mice through surgical destabilization of the medial meniscus (DMM) in the right knee joint. Subsequently, from week 13 onwards, JP4-039 (10 μM) was administered intra-articularly into the right knee joint three times per week, and the dose for each injection is 8 μl. The mice at 12 weeks of age were randomly assigned to four groups: (1) Sham surgery (Sham); (2) Sham with JP4-039 treatment; (3) DMM surgery; (4) DMM with JP4-039 treatment; In the Sham and DMM groups, mice received an injection of 8 μL normal saline.

2.4. DMM-induced OA mouse model

The surgically induced osteoarthritis (OA) model through destabilization of the medial meniscus (DMM) was established following previously documented procedures [24]. Under isoflurane anesthesia, the right knee joint, 12-week-old male C57BL/6 mice was surgically prepared. The skin was sterilized, dissected layer by layer up to the inside of the joint capsule at the medial site of the patellar ligament, exposing the medial meniscus and subsequently resecting the transverse knee ligament. Suturing and re-sterilization with iodophor followed. The sham-operated group involved skin incision without ligament dissection, followed by suturing.

2.5. Open field test (OFT)

The autonomous activity of the mice was evaluated utilizing an animal tracking system (Zhenghua Technology, China). Each mouse was

systematically introduced into an unilluminated 50 × 50 cm indoor arena. Real-time tracking via a camera was conducted for a 3-min interval, with subsequent recordings facilitating the assessment of key parameters, including distance traveled, relative activity, activity duration, and average speed.

2.6. Footprint experiment

Mice were undergone gait analysis by applying red and blue ink to their front and back paws, respectively. The mice freely walked on a 70 cm × 20 cm track covered with white paper. The inked footprints on the paper were utilized to assess relative stride lengths, step lengths, and front and back paw distances. The procedure, conducted in a dim and quiet environment, involved at least three trials per mouse, ensuring the safety and non-toxicity of the ink.

2.7. Von Frey fiber test

Mechanical pain experiments were conducted employing an electronic von Frey Anesthesiometer (IITC, Woodland Hills, USA). Each mouse was acclimated to a cage with a 4 cm × 3 cm x 7 cm wire mesh bottom for 15 min before von Frey fibers were applied to the right hind paw. The force was gradually increased until the mice exhibited pain, as indicated by the withdrawal of their right paw [25]. The lower the withdrawal threshold, the greater the sensitivity to pain. Experimental subjects were blinded to the grouping, minimizing subjective factors.

2.8. Extraction of human OA tissue protein

Following morphological and histological characterization of intact and damaged areas, human osteoarthritis (OA) cartilage was finely sectioned and pulverized under liquid nitrogen. The resulting cartilage powder was homogenized with cold saline, and the supernatant was extracted post-centrifugation (12,000 rpm, 20 min, 4 °C).

2.9. Histological analysis

After decalcified by 10 % EDTA (#1340, Biofroxx, Germany) solution, Human cartilage and mouse knee joints underwent gradient dehydration and were paraffin-embedded. Coronal sections (5 μm) were obtained using a paraffin slicer (Thermo, Germany). Following a previously reported procedure, 15 every fifth section of two slides were selected and stained with Safranin-O/fast green (S.O.) (#G1371, Solarbio, Beijing, China) and hematoxylin and eosin (H&E) (#C0105S, Beyotime) to evaluate the cartilage lesions and synovitis, respectively. Severity of osteoarthritis (OA) was assessed by blinded observers using the OARSI scoring system (0–6 points), and synovitis was scored on a 0–3 point scale. Scores were recorded for each section, and the mean score was calculated as previously described.

2.10. Immunofluorescence (IF) staining

Deparaffinization and hydration of mouse knee joint sections and Human cartilage were accomplished using xylene and a gradient of alcohol. Antigenic retrieval was performed using pepsin at 37 °C for 1 h. Following washing with phosphate-buffered saline (PBS), the tissues were subsequently blocked with 5 % bovine serum albumin (BSA) for 1 h at 37 °C. Subsequently, the sections were incubated overnight at 4 °C with primary antibodies (dilution 1:200) against Parkin (#GB113802-100, Servicebio), Pink1 (#23274-1-AP, Proteintech), Tomm20 (#66777-1-lg, Proteintech) Mmp13 (#GB11247, Servicebio), Cox2 (#12282, Cell Signaling Technology), Gpx4 (#A11243, ABclonal), FTH1 (#4393, Cell Signaling Technology), and Ncoa4 (#66849, Cell Signaling Technology). Following three washes with TBST, the sections were treated with a fluorescein isothiocyanate (FITC)-conjugated secondary antibody for 1 h at 37 °C. After staining the nuclei with 2-(4-Amidinophenyl)-6-indolecarbamidine dihydrochloride (DAPI), immunofluorescence images were captured using a fluorescence microscope (Zeiss, Germany).

2.11. Immunohistochemical (IHC) staining

Following deparaffinization and hydration, the tissue sections underwent an initial immersion in a 3 % H_2O_2 solution to neutralize endogenous peroxidase activity under light protection. Subsequent to washing with PBS, antigenic retrieval was performed using pepsin at 37 °C for 1 h. Subsequently, the sections were incubated with 5 % BSA for 1 h and then exposed to primary antibodies against Col II (#BA0533, Boster) and 4-HNE (#ab46545, Abcam) overnight at 4 °C. Following this, the horseradish peroxidase (HRP)-coupled secondary antibody was applied at room temperature for 1 h. Color development was achieved using the ultra-sensitive DAB kit (#1205250, Typing). After hematoxylin staining for nucleus visualization, the sections were sealed with resin.

2.12. Micro-computed tomography (micro-CT) analysis

Before histologic examination, mouse knee joints underwent assessment with a Swiss VivaCT 80 scanner (Scanco Medical AG) at a resolution of 18.38 μm. Three-dimensional reconstructions of the joints were generated using Scanco medical software. Analysis of the cancellous bone aimed to derive trabecular-related parameters, subchondral bone volume, and quantify the number of bone fragments and subchondral bone thickness for each knee joint through 3D reconstruction. Analysis of the subchondral bone of the medial femoral condyle from the distal edge of the epiphysis by a blind observer 20 layers. The thickness of the subchondral plate is calculated by multiplying the number of cross-sections forming the subchondral plate with the thickness of the cross-sections [26].

2.13. Cell culture

Primary mouse chondrocytes were harvested and cultured following established procedures. In brief, rib cartilage obtained from 3-day-old C57BL/6 mice was dissected and digested with 4 mL of 0.2 % Collagenase 2 (Gibco, USA) for 4 h at 37 °C. After removing soft tissues, chondrocytes were cultured in Dulbecco's modified Eagle's medium containing 1 g/L glucose (Gibco, Carlsbad, CA), supplemented with 10 % fetal bovine serum (Gibco) and 1 % penicillin and streptomycin (Gibco) under conditions of 37 °C and 5 % CO_2. The cell culture medium was refreshed every 72 h. Chondrocytes were subjected to treatments with TBHP (#MKCH9944, Sigma, USA), 10 μM JP4-039 (1205492-16-5, Sigma), and 50 μM Mdivi-1 (HY-15886, MCE-MedChemExpress) as indicated. For the solubilization of the drug, we used DMSO (200-664-3, Sigma) solubilization. And we also added an equal amount of DMSO in the control group to maintain the consistency of the drug's dissolution mode on the cells.

2.14. Protein extraction and western blot

Total protein extraction from human cartilages and chondrocytes subjected to various treatments was performed using RIPA lysis buffer (#R0010, Solarbio) supplemented with 1 mM phosphatase inhibitor cocktail (#B15002, Bimake, USA) and 1 mM phenylmethanesulfonyl fluoride (#329-98-6, Solarbio). Western blot analysis was carried out following established protocols. The primary antibodies included Collagen II (#BA0533, Boster), Collagen I (#ab138492, Abcam), NCOA4 (#66849, Cell Signaling Technology), COX2 (#12282, Cell Signaling Technology), FTH1 (#4393, Cell Signaling Technology), FSP1 (#24972, Cell Signaling Technology), MMP13 (#ab219620, Abcam), Parkin (#ab77924, Abcam), Pink1 (#23274-1-AP, Proteintech), GPX4 (#ab125066, Abcam), and β-ACTIN (#5795, Cell Signaling

Technology). Following incubation with horseradish peroxidase-conjugated goat anti-rabbit/mouse secondary antibodies (#BL003A or #BL001A, Biosharp), western blots were visualized using the Chem-iDocXRS + Imaging System (Tanon, Shanghai, China). Quantitative protein analysis was performed using Image J (version 1.8.0). All antibodies utilized in this study were commercially sourced.

2.15. Quantitative real-time polymerase chain reaction (qPCR)

Cellular mRNA was extracted employing the RNA-quick Purification Kit (#RN001, ES Science, Shanghai, China), and quantitative polymerase chain reaction (qPCR) was performed using the SYBR Green Q-PCR Kit (#Q411-02, Vazyme, Nanjing, China) on a Light Cycler 480 PCR System (Roche, Switzerland). The primer sequences used are listed in Supplementary Table 1.

2.16. Cell counting Kit-8 (CCK-8) assay

Primary mouse chondrocytes were obtained from the rib cartilage of C57BL/6 mice within 3 days of birth. Cells were cultured in DMEM/F12 medium (Gibco) supplemented with 1 % penicillin and streptomycin, along with 10 % fetal bovine serum (Gibco), under standard conditions of 37 °C and 5 % CO2. Inoculate chondrocytes into a 96-well plate, expose to various concentrations of JP4-039 (Sigema, 1205492-16-5) for 24 h to assess drug toxicity. Within the established toxicity range, co-incubate cells with varying concentration gradients of JP4-039 and TBHP for 24 h to determine the drug's maximum effective concentration. Cell viability was assessed utilizing a CCK-8 assay (#CK04, Dojindo) following the manufacturer's instructions.

2.17. Cell probe fluorescence

Intracellular levels of reactive oxygen species (ROS), lipid peroxidation, and Fe^{2+} accumulation were assessed using 10 mM ROS probe DCFH-DA (#S0033S, Beyotime), 5 mM lipid ROS probe C11-BODIPY 581/591 (#GC40165, GLPBIO, USA), and 1 mM Fe^{2+} probe FerroOrange (#F374, Dojindo, Japan), respectively. In order to observe changes in mitochondrial autophagy, Mito-Tracker Deep Red FM (#C1032, Beyotime), which allows observation of mitochondria, was loaded and co-incubated with Lyso-Tracker Green (#C1047S, Beyotime), which allows localization of lysosomes, and pEGFP-C3-MAP1LC3B (Biogot Biotechnology, China), which allows localization of autophagic vesicles, respectively. Following overnight starvation, chondrocytes were subjected to a 30-min incubation with probes at 37 °C, followed by treatment with 100 μM TBHP, with or without 10 μM JP4-039, for 4 h. The final fluorescence intensity was observed at different wavelengths in the fluorescence microscope.

2.18. Statistical analysis

Statistical analyses were conducted using SPSS software (version 25.0) and GraphPad Prism software (version 8.0). Quantitative data represent a minimum of three independent experiments, with no exclusion of samples or animals during analysis. The Shapiro–Wilk test and Levene method were applied to assess data normal distributions and homogeneity of variance, respectively. Paired or unpaired two-tailed Student's t-test was employed for comparing mean values between two groups. One-way or two-way analysis of variance (ANOVA) followed by Tukey's post-hoc tests were utilized to evaluate the statistical significance of mean values across more than two groups. Data were expressed as mean values ± standard deviation (SD), and statistical significance was set at $P < 0.05$.

3. Results

3.1. Ferroptosis in osteoarthritis cartilage is linked with a reduction in mitophagy

To investigate the relationship between ferroptosis and mitophagy in osteoarthritis (OA), our study involved analyzing specific markers in both intact and damaged OA cartilage areas. Using morphological and histological staining techniques, we differentiated non-injured and injured cartilage regions (Fig. 1a, b, f). Our findings showed decreased levels of GPX4 (an iron death-related marker) and increased levels of COX2 (associated with ferroptosis) in the injured cartilage (Fig. 1c, d, f), indicating increased ferroptosis in OA damaged regions. Additionally, we observed reduced expression of PARKIN and PINK1 (linked to mitophagy) in the damaged cartilage (Fig. 1e and f), indicating a decrease in mitophagy. Consistent with these observations in intact versus injured cartilage, we replicated similar decreases in mitophagy-associated markers Parkin and Pink1 in DMM mice, supporting our findings regarding the relationship between ferroptosis and reduced mitophagy in OA (Supplementary Figs. 1a–c).

In our investigation of intact versus damaged cartilage, distinct protein expression patterns emerged. Damaged cartilage displayed heightened levels of COL I alongside reduced COL II, along with elevated MMP13 levels indicating cartilage degradation. Additionally, increased COX2 and decreased GPX4 and FTH1 indicated heightened ferroptosis in the injured chondrocytes. Furthermore, diminished expression of PARKIN and PINK1 proteins associated with mitophagy suggested a decline in this cellular cleansing process (Fig. 1g and h). Our correlation analysis unveiled a negative relationship between ferroptosis in damaged chondrocytes and mitophagy, shedding light on a potential interplay between these mechanisms impacting cartilage health (Fig. 1i). This suggests that mitophagy dysfunction may lead to chondrocyte ferroptosis.

3.2. JP4-039 exhibits an anti-ferroptotic effect in chondrocytes

Based on our findings, we identified JP4-039 as a potential therapeutic agent for preventing chondrocyte ferroptosis and restoring mitochondrial function due to its antioxidant properties and mitochondrial targeting abilities (Fig. 2a).

We simulated chondrocyte ferroptosis using TBHP (50 μM) on primary mouse chondrocytes. We tested JP4-039 for its toxicity and effectiveness. To ensure JP4-039 itself didn't impact cell viability, we incubated chondrocytes with various JP4-039 concentrations, finding no significant change in viability below 50 μM (Fig. 2b). TBHP stimulation also didn't notably affect cell viability. Post-TBHP stimulation, incubating with different JP4-039 concentrations revealed viability plateauing at 10 μM (Fig. 2c). Hence, 10 μM was chosen as the effective JP4-039 concentration. Unexpectedly, scratch experiments revealed that JP4-039 had some migration-promoting effects on chondrocytes (Supplementary Fig. 2).

To examine JP4-039 impact on chondrocyte ferroptosis we used specific probes for intracellular ferrous ions (Ferro Orange), ROS (DCFH-DA), and lipid peroxidation (C11-BODIPY). TBHP notably increased ferrous ion levels, ROS, and lipid peroxidation, all significantly curbed by JP4-039 (Fig. 2d, e, g). This suggests JP4-039 effectively mitigated TBHP-induced markers of ferroptosis in chondrocytes. Additionally, JC-1 probe revealed JP4-039's ability to alleviate TBHP-induced damage to mitochondrial membrane potential (CCCP, a drug that induces depolarization of mitochondrial membrane potential, was used here as a positive control group) (Fig. 2f and g). Electron microscopy displayed altered mitochondrial morphology in TBHP-stimulated chondrocytes, featuring swelling and loss of cristae, indicative of mitochondrial damage. JP4-039 administration reversed these changes caused by ferroptosis (Fig. 2h).

Then, we delved into chondrocyte gene expression related to anabolism, catabolism, and ferroptosis. TBHP stimulation led to heightened

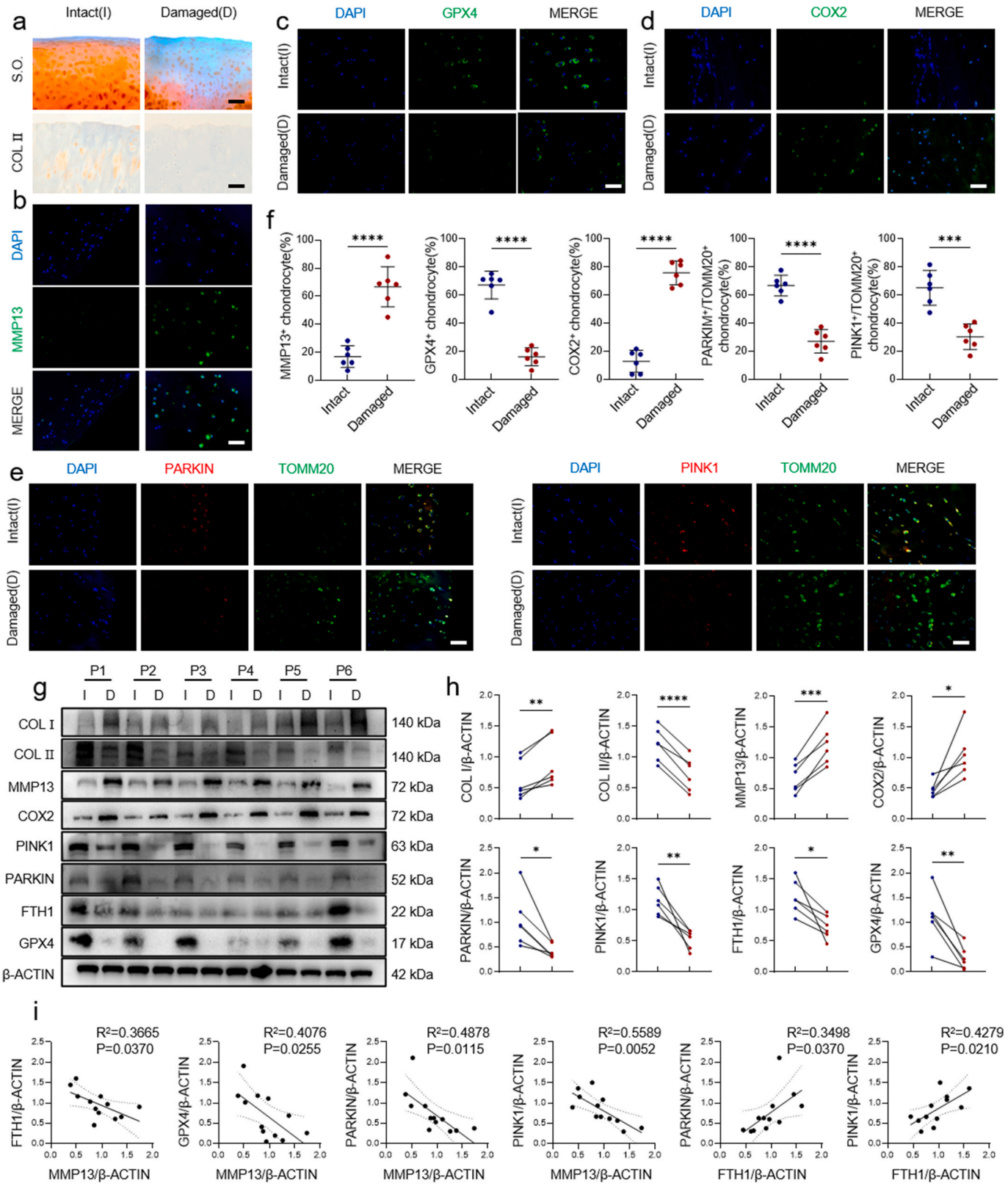

Fig. 1. Ferroptosis traits in OA showed an inverse correlation with reduced mitophagy. (a) Safranin O-Fast Green (S.O) staining of both intact (I) and damaged (D) articular cartilages retrieved from OA patients; Immunohistochemical (IHC) staining of Collagen II (COL II) in human OA cartilages. (b–e) Immunofluorescence (IF) staining of MMP13, GPX4, COX2, PARKIN and PINK1 in human OA cartilage. (f) t-test. Data are shown as mean ± SD. (g–h) Western blot analysis and quantification of indicated proteins in paired intact (I) and damaged (D) (n = 6) human OA cartilages, including a correlation analysis. Scale bars, 50 μm (a–e). Data are shown as mean ± SD. *p < 0.05; **p < 0.01; ***p < 0.001

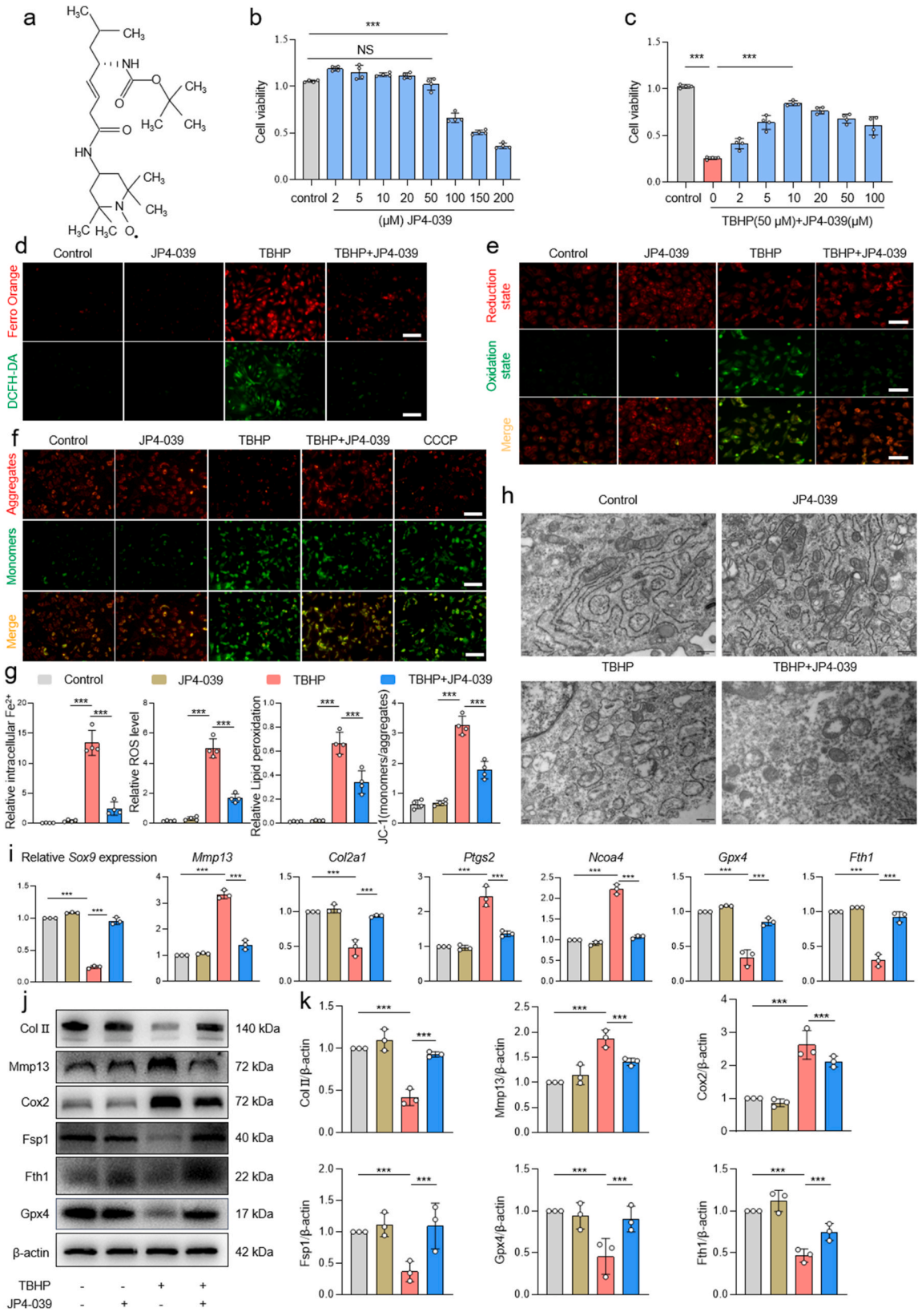

Fig. 2. JP4-039 inhibits chondrocyte ferroptosis. (a) Molecular formula of the drug JP4-039. (b, c) CCK-8 assay for the toxicity and potency of JP4-039. (d–g) Fluorescence detection of intracellular reactive oxygen species, ferrous ions, lipid peroxidation and mitochondrial membrane potential depolarization probes and corresponding statistical analysis. Scale bars, 100 μm (h) Mitochondria of chondrocytes photographed by projection electron microscopy. (i) qPCR analysis of indicated genes in chondrocytes treated with 50 μM TBHP an/or 10 μM JP4-039 for 6 h (n = 3). (j, k) Western blot analysis was performed on indicated proteins in mouse primary chondrocytes treated with 50 mM TBHP and/or 10 μM JP4-039 for 6 h. Data are shown as mean ± SD. *p < 0.05; **p < 0.01; ***p < 0.001.

expression of *Gpx4* and *Fth1* (ferroptosis suppressors) alongside increased *Ptgs2* and *Ncoa4* (ferroptosis promoters) genes, indicating induced ferroptosis in chondrocytes. Additionally, *Mmp13* (a catabolic indicator) surged while *Col2a1* and *Sox9* (anabolic indicators) decreased (Fig. 2i). These results suggested JP4-039's protective role by hindering chondrocyte ferroptosis. Further, we explored JP4-039's impact on chondrocyte ferroptosis at the protein level. JP4-039 significantly countered TBHP-induced reduction in Col2a1 protein synthesis and the rise in Mmp13 expression caused by chondrocyte ferroptosis. TBHP reduced levels of ferroptosis suppressor proteins (Gpx4, Fth1, Fsp1), which were notably restored by JP4-039 treatment. Cox2, an ferroptosis driver protein, rose post-TBHP but significantly decreased after JP4-039 administration (Fig. 2j and k). These findings collectively indicated JP4-039's ability to alleviate TBHP-induced chondrocyte ferroptosis.

3.3. JP4-039 protects chondrocytes from ferroptosis in OA

In order to further clarify whether JP4-039 can inhibit the occurrence of chondrocyte ferroptosis, thereby protecting cartilage and delaying the pathological progression of OA, we constructed a mouse OA model using DMM surgery and performed intra-articular injections of JP4-039 in order to evaluate its regulatory effect on the progression of OA in mice. The Safranin-O/fast green (S.O.) staining and the hematoxylin & eosin (H&E) staining results showed that JP4-039 treatment demonstrated significant chondroprotective effects, including a reduction in cartilage number loss and Osteoarthritis Research Society International (OARSI) scores (Fig. 3a–c). In addition, in the JP4-039-treated DMM surgical group, an increase in Col II^{+} regions as well as Aggrecan^{+} chondrocytes, suggestive of cartilage anabolism, and a

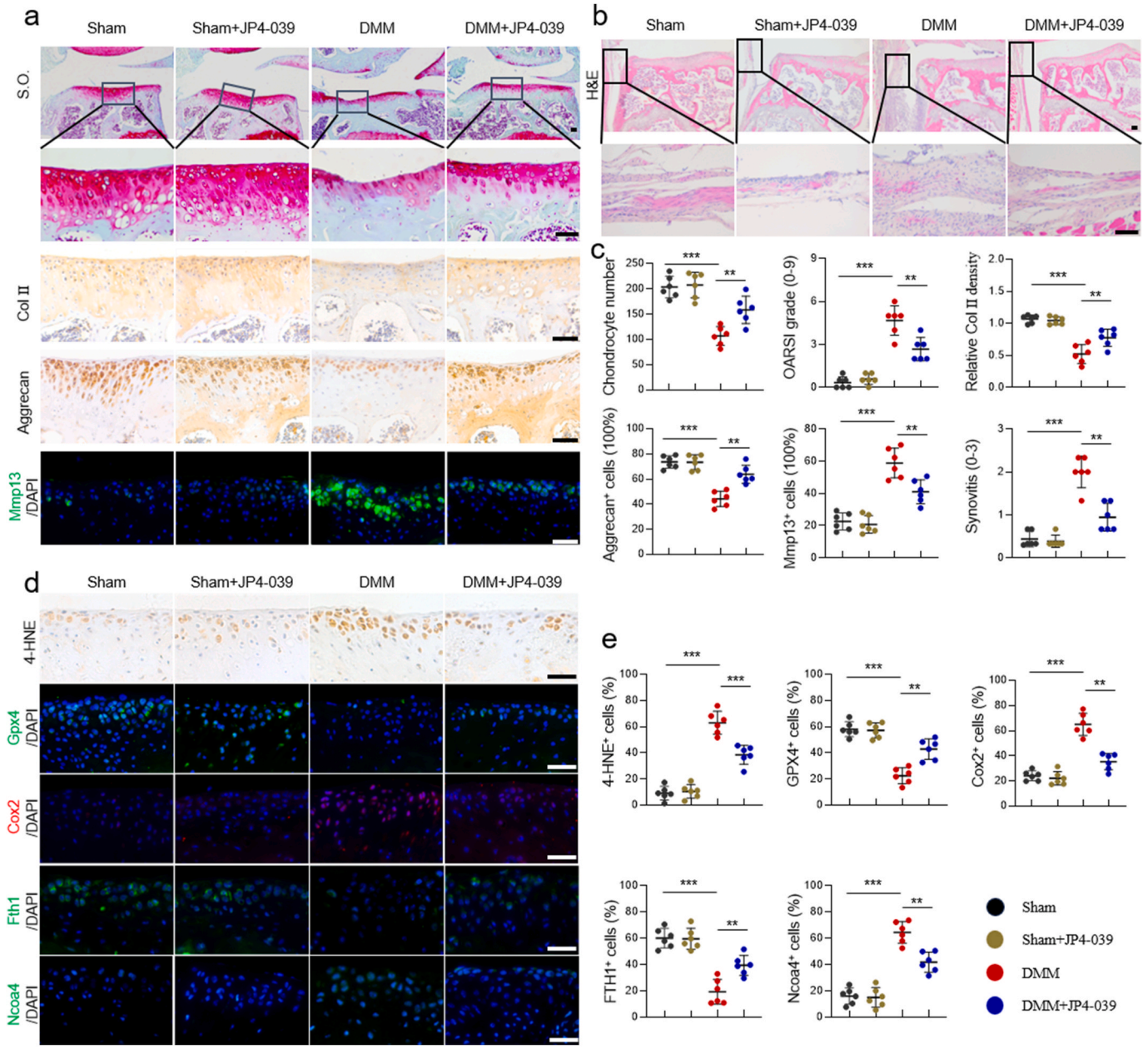

Fig. 3. JP4-039 delays OA by inhibiting chondrocyte ferroptosis. (a) Safranin-O/fast green (S.O.) staining; Immunohistochemical (IHC) staining of Col II and Aggrecan; Immunofluorescence (IF) staining of Mmp13 (n = 6). (b) Hematoxylin & Eosin (H&E) staining of mice knee (c) The quantification of S.O., Col II, Aggrecan and Mmp13 (n = 6). (d) Immunohistochemical (IHC) staining of 4-HNE; Immunofluorescence (IF) staining of Gpx4, Cox2, Fth1, Ncoa4 (n = 6). (e) The quantification of Gpx4, Cox2, Fth1, Ncoa4 (n = 6). Scale bars, 50 μm. One-way ANOVA with Tukey's post-hoc test. Data are shown as mean ± SD. *p < 0.05; **p < 0.01; ***p < 0.001.

decrease in $Mmp13^{+}$ chondrocytes, suggestive of a decrease in cartilage catabolism, were observed (Fig. 3a–c).

Further, in the OA mouse model, the impact of JP4-039 on chondrocyte ferroptosis was further assessed. Immunofluorescence staining of knee joint tissues revealed that JP4-039-treated DMM mice exhibited a notably reduced presence of 4-HNE^{+}, $Cox2^{+}$, and $Ncoa4^{+}$ chondrocytes in the cartilage. This reduction suggests a significant inhibition of chondrocyte ferroptosis by JP4-039. Additionally, JP4-039 demonstrated an inhibitory effect on the decline of ferroptosis suppressor genes Gpx4 and Fth1 (Fig. 3d and e). These findings underscore JP4-039's potential in effectively restraining chondrocyte ferroptosis cell death in the context of osteoarthritis.

3.4. JP4-039 improves bone remodeling and behavioral performance in DMM mice

It has been concluded that abnormal bone remodeling is a major pathological feature of OA, including osteophytes formation and subchondral bone sclerosis. Based on these results, JP4-039 could exert chondroprotective effects by inhibiting chondrocyte ferroptosis, and we next further analyzed the effects on abnormal bone remodeling. We used micro-CT scanning analysis and 3D reconstruction, and found that the DMM modeled mice showed obvious bone recumbency around the knee joint and subchondral bone thickening, and the subchondral bone microstructure of the knee joint was obviously changed. Meanwhile, the bone volume (BV), bone mineral density (BMD), bone volume/tissue volume (BV/TV), trabecular thickness (Tb.Th), and trabecular number (Tb. N) of the knee joints of the DMM-modeled mice were all significantly higher than in the sham group, while trabecular separation (Tb. Sp) was significantly reduced. Meanwhile, we found that after modeling of mouse knee DMM, intra-articular administration of JP4-039 was able to significantly reduce the number of osteophyma and decrease the thickness of subchondral bone, as well as decrease the knee BV, BV/TV, subchondral bone BMD, Tb.Th, and Tb.N, and elevate the Tb.Sp (Fig. 4a–c). These results suggested that JP4-039 significantly improves the abnormal bone in the mouse model of DMM remodeling.

The above results indicated that JP4-039 had an overall protective effect on OA, so we next further analyzed the activity of the mice through behavioral experiments to reflect the knee joint function. We first evaluated the effects of the drug on the body weight, knee swelling, and pain threshold of the mice, and the results showed that JP4-039 had no significant effect on the body weight of the mice, and that JP4-039 improved knee swelling in DMM mice as measured by the knee joint diameter, and the von Frey fiber test also showed that the paw withdrawal threshold of the mice also increased significantly after treatment, which reflected the increase in pain threshold of mice (Fig. 4d). Next, mice underwent an open field test (OFT) to monitor their spontaneous activity for a duration of 3 min. Through the results we can observe that DMM mice showed a significant decrease in relative mobility, activity time, activity distance and average speed, which was significantly reversed after receiving treatment with knee injections of JP4-039 (Fig. 4e and f). Additionally, we reinforced our assessment of pain and gait conditions through footprint experiments. The results showed that JP4-039 significantly reduced pain and improved locomotor trajectory in mice, which was mainly reflected in the improvement of step length and stride length, as well as the shorten of the front/rear print length (Fig. 4g and h). In summary, JP4-039 significantly improved physical activity in mice.

Furthermore, H&E staining of the heart, liver, spleen, lung, and kidney tissues revealed no discernible structural or cellular distinctions among the groups. These findings affirm that JP4-039 exhibits no apparent signs of toxicity (Supplementary Fig. 3).

3.5. JP4-039 promotes Pink1/Parkin-dependent mitophagy

The obtained experimental findings indicate that JP4-039 has the potential to impede chondrocyte ferroptosis, thereby potentially decelerating the progression of osteoarthritis. The subsequent phase involves investigating whether JP4-039 can enhance mitophagy in chondrocytes to counteract the inhibition of ferroptosis. Mitophagy encompasses diverse yet interconnected mechanisms, typically classified into Ub-dependent and Ub-independent pathways. Among the Ub-dependent pathways, the Pink1/Parkin pathway stands as one of the most prevalent. Hence, our subsequent investigations primarily centered on elucidating the Pink1/Parkin-dependent pathway of mitophagy. Initially, we assessed the expression of Pink1 and Parkin at both gene and protein levels. Findings indicated a declining trend in mitophagy-associated Pink1 and Parkin expression upon TBHP induction, suggesting a concurrent reduction in mitophagy during the ferroptosis process. Interestingly, supplementation with JP4-039 notably ameliorated this declining trend in Pink1 and Parkin, specifically associated with mitophagy (Fig. 5a–c). To validate Pink1 and Parkin expression levels, immunofluorescence staining was conducted on the DMM mouse model. Results revealed notable downregulation of Pink1 and Parkin expression in cartilage, a trend significantly reversed upon JP4-039 treatment (Fig. 5d–f). These observations align with in vitro murine chondrocyte cultures, further indicating JP4-039's capacity to modulate chondrocyte mitophagy.

When mitochondria initiate autophagic signaling, autophagosomes wrap around mitochondria to become mitochondrial autophagosomes. Lysosomes bind to mitochondrial autophagosomes, thereby promoting the degradation of mitochondrial content. Therefore, we used, Mito-Tracker Deep Red FM, Lyso-Tracker Green and pEGFP-C3-MAP1LC3B to localize mitochondria, lysosomes and autophagosomes respectively, and co-localized staining of mitochondria with lysosomes and autophagosomes respectively. The results showed that the co-localization of lysosomes and mitochondria, autophagic vesicles and mitochondria showed a decreasing trend after the addition of TBHP, which indicated that the occurrence of ferroptosis in chondrocytes was accompanied by a decrease in mitophagy (Fig. 5g). And the co-localization increased after treatment with JP4-039, which indicated that JP4-039 could reverse the trend of decreased mitophagy.

3.6. Inhibited mitophagy weakens JP4-039's anti-ferroptotic impact on chondrocytes

The above results indicated that JP4-039 could promote mitochondrial autophagy in chondrocytes. In order to further verify whether ferroptosis could be inhibited by restoring mitophagy and thus slowing down the progression of osteoarthritis, we used Mdivi-1, a mitophagy inhibitor, to validate the mechanism of JP4's action in the fight against chondrocyte ferroptosis. First, we first verified the efficacy of Mdivi-1 in inhibiting mitophagy. After the addition of the inhibitor Mdivi-1, mitophagy-associated Pink1 as well as Parkin were markedly inhibited at the gene as well as protein level (Fig. 6a and b). We detected the cell activity by CCK-8 assay, which showed that there was no difference between the cell activity after the addition of Mdivi-1 and the TBHP group alone, and the cell activity could be restored after the addition of JP4-039 again (Supplementary Fig. 4).

Next, the mitophagy inhibitor Mdivi-1 was added to JP4-039-treated chondrocytes, and anabolism, catabolism, and ferroptosis-related genes were examined in chondrocytes. The results showed that the up-regulation of the ferroptosis protective genes *Gpx4* and Fth1 and the down-regulation of the ferroptosis driver genes *Ptgs2* and *Ncoa4* by JP4-039 were significantly antagonized by the inhibitor, and the increase in the expression of the chondrocyte anabolic genes *Col2a1* and *Sox9* induced by JP4-039 was also significantly inhibited, and that the expression of the catabolic gene *Mmp13* was significantly inhibited by the addition of Mdivi-1(Fig. 6c). These indicate that the anti-chondrocyte ferroptosis function of JP4-039 was significantly suppressed. Similarly, the results at the protein level of chondrocytes showed that after the addition of Mdivi-1, the cartilage anabolic index,

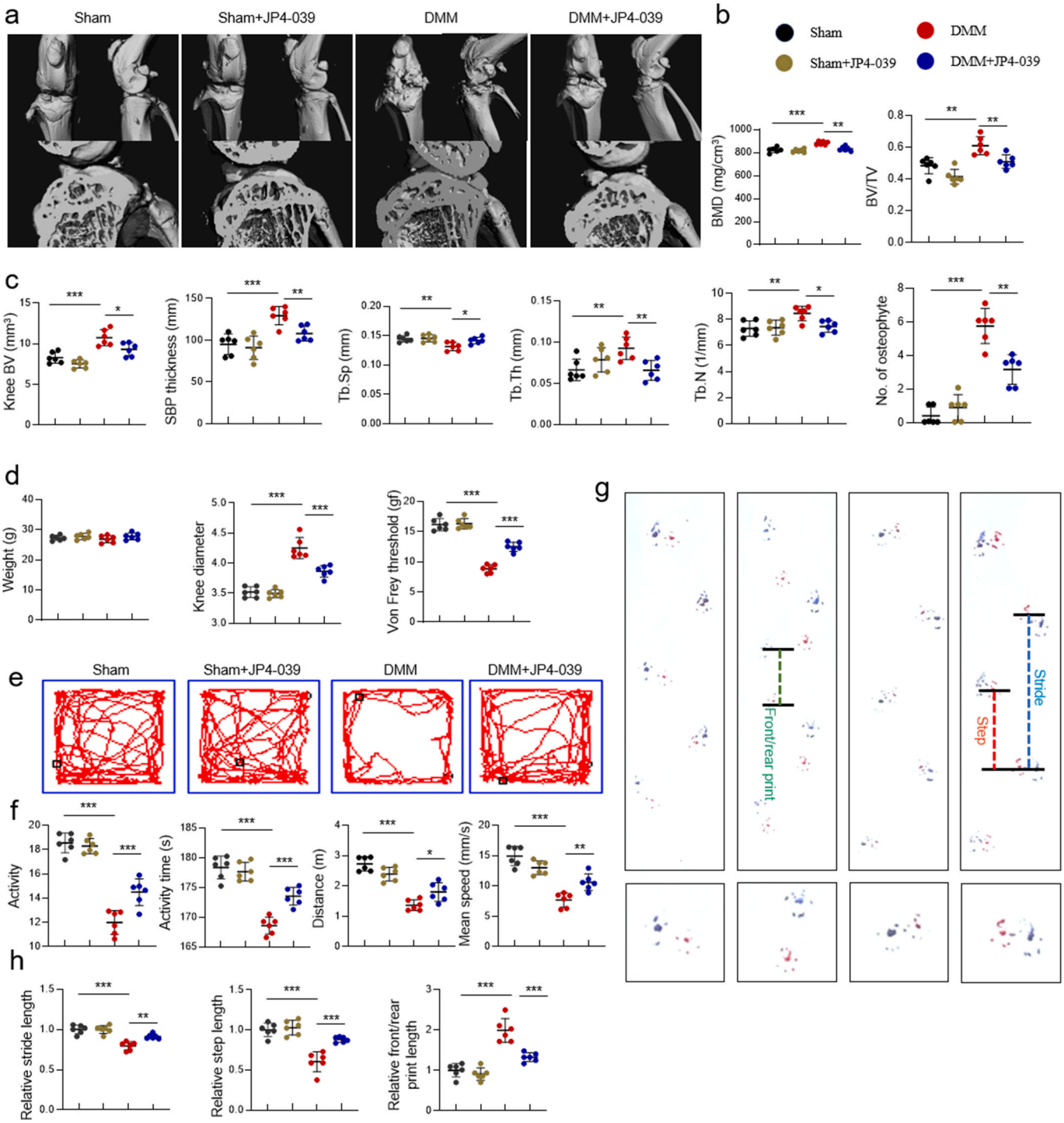

Fig. 4. JP4-039 enhances bone remodeling and cognitive performance in DMM mouse. (a) Micro-computed tomography (micro-CT) was employed to reconstruct three-dimensional images of the mouse knee joint, emphasizing alterations in both femoral and tibial surfaces, with a focus on minimizing repetition(n = 6). (b, c) Quantified changes in BMD, BV/TV, BV, SBP, Tb.Sp, Tb.Th, Tb.N, No.of osteophyte(n = 6). One-way ANOVA with Tukey's post-hoc test. (d) The quantification of mice weight and Knee diameter(n = 6); Paw contraction thresholds were assessed utilizing von Frey fibers to gauge mechanical sensitivity, with an emphasis on reducing redundancy(n = 6). (e) Representative trajectory plots reveal a reduction in spontaneous activity of mice following DMM surgery during the open field test, highlighting a decrease without unnecessary repetition. (f) Alterations in spontaneous activity, encompassing relative activity, active time, distance covered, and mean speed, were examined with an effort to minimize redundancy(n = 6). (g, h) The JP4-039 treatment group exhibited increased relative step length and relative stride length, while concurrently demonstrating a reduction in relative front/rear print length in DMM mice, with a focus on minimizing repetitive language(n = 6). Scale bars, 50 μm One-way ANOVA with Tukey's post-hoc test. Data are shown as mean ± SD. *p < 0.05; **p < 0.01; ***p < 0.001.

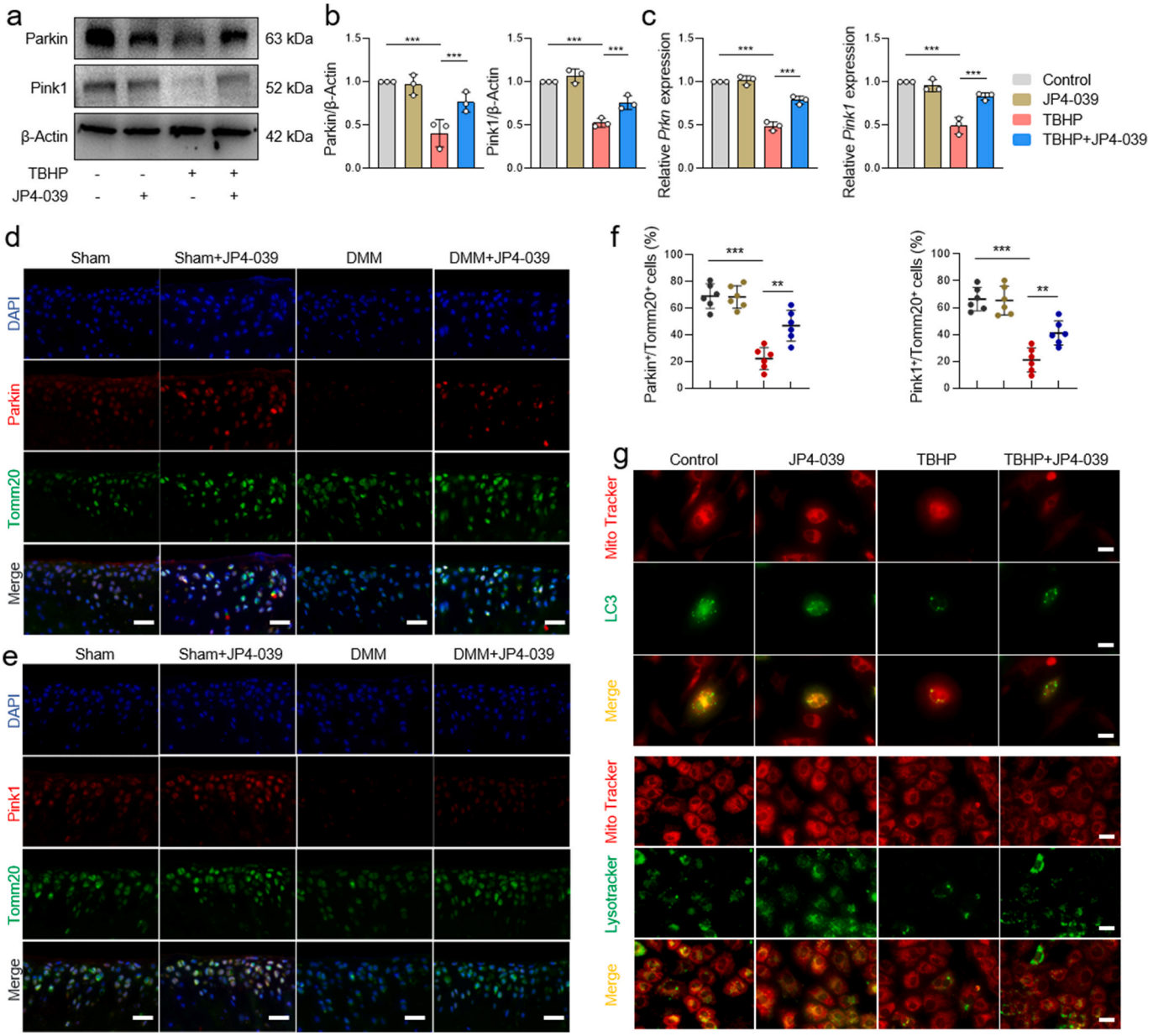

Fig. 5. JP4-039 Promoting mitophagy to inhibit ferroptosis. (a, b) Western blot analysis was performed on indicated proteins in mouse primary chondrocytes treated with 50 mM TBHP and/or 10 μM JP4-039 for 6 h (n = 3). (c) qPCR analysis of indicated genes in chondrocytes treated with 50 μM TBHP an/or 10 μM JP4-039 for 6 h (n = 3). (d) Immunofluorescence (IF) staining of Parkin and Tomm20 (n = 6). (e) Immunofluorescence (IF) staining of Pink1 and Tomm20 (n = 6). (f) The quantification of Parkin and Pink1. (g) Mito-Tracker Deep Red FM was co-incubated with Lyso-Tracker Green and pEGFP-C3-MAP1LC3B, respectively in chondrocytes treated with 50 μM TBHP an/or 10 μM JP4-039 for 6 h (n = 3). Scale bars, 50 μm. Data are shown as mean ± SD. *p < 0.05; **p < 0.01; ***p < 0.001

Col2a1, was significantly decreased, the catabolic index, Mmp13, was significantly increased, and the expression of the ferroptosis driving protein, Cox2, was increased, and the expression of the ferroptosis inhibitory proteins, Gpx4, and Fth1, was decreased, which was in line with the results at the gene expression level (Fig. 6d and e). Taken together, these results all indicate that the inhibition of mitophagy blocked the anti-chondrocyte ferroptosis effect of JP4-039. Mitochondria serve as intracellular storage organelles for ROS, and imbalance in mitochondrial homeostasis leads to intracellular ROS accumulation. Our experimental results indicate that the addition of Mdivi-1 leads to cellular ROS accumulation (Supplementary Fig. 5).

4. Discussion

Chondrocyte ferroptosis and mitophagy influence the progression of osteoarthritis (OA). However, the intricate link between dysfunctional mitophagy and chondrocyte ferroptosis remains unclear. This study aimed to elucidate the relationship, highlighting decreased mitophagy in chondrocytes as a driving force for ferroptosis, thus establishing it as a promising therapeutic target. Our focus pivoted towards reestablishing mitophagy while mitigating ferroptosis. A key avenue was the targeting of intracellular oxidative stress and precise mitochondrial intervention, leading to the identification of JP4-039 as a potential therapeutic agent. Experimental findings unveiled a reduction in the expression of mitophagy-associated proteins Pink1 and Parkin in TBHP-induced chondrocyte ferroptosis. This decline suggested a concurrent decrease in mitophagy alongside chondrocyte ferroptosis. However, upon JP4-039 treatment, a notable inhibition of chondrocyte ferroptosis coupled with effective restoration of mitophagy levels was observed. Immunofluorescence staining of knee joints in OA mice further corroborated

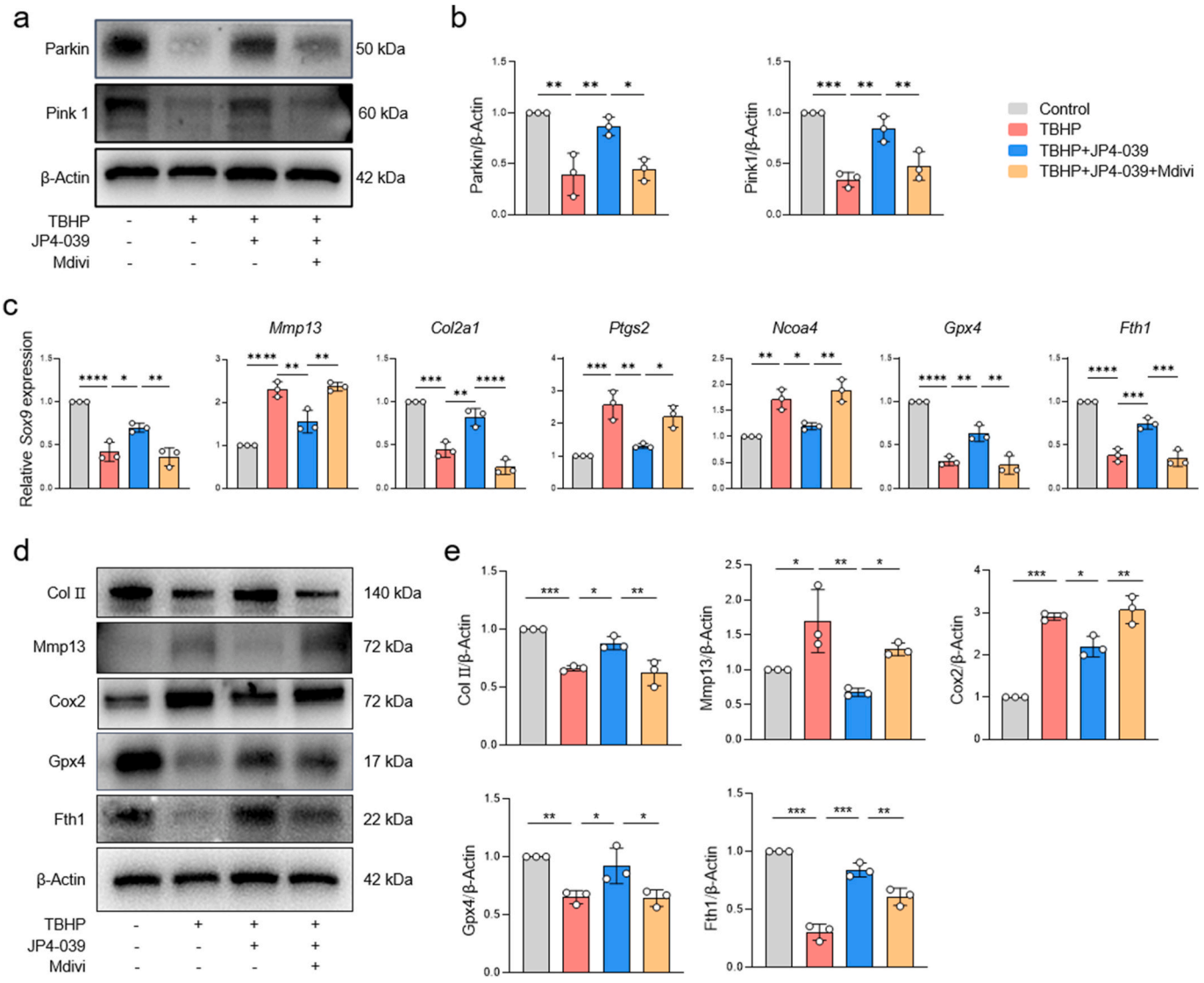

Fig. 6. Inhibition of mitophagy counteracts the anti-ferroptosis function of JP4-039. (a, b, d) Western blot analysis was performed on indicated proteins in mouse primary chondrocytes treated with 50 mM TBHP and/or 10 μM JP4-039 and Mdivi-1 for 6 h(n = 3). (c) qPCR analysis of indicated genes in chondrocytes treated with 50 μM TBHP an/or 10 μM JP4-039 and Mdivi-1 for 6 h (n = 3). Data are shown as mean ± SD. *p < 0.05; **p < 0.01; ***p < 0.001. (E)Western blot analysis of protein expression and quantification of Col II, Mmp13, Cox2, Gpx4 and Fth1 in different groups (n=3).

these results, demonstrating reduced mitophagy in OA cartilage. Notably, treatment with JP4-039 significantly restored Pink1 and Parkin levels in mouse cartilage, mirroring outcomes observed in our in vitro TBHP-induced chondrocyte model. This collective evidence strongly supports JP4-039's capacity to curtail chondrocyte ferroptosis by reinstating mitophagy. Interestingly, in vitro tests revealed that subchondral osteosclerosis was improved in DMM mice after injection of JP4-039 into the knee joint. This could be a direct effect of the drug or an indirect effect that affects the chondrocyte state, and we are still working on the direct effect, whereas on the indirect effect, there are studies that show that there is an interaction between the chondrocyte state and the subchondral bone. It is now well documented that there is a correlation between cartilage degeneration and subchondral bone sclerosis in OA, with chondrocytes releasing exosomes that lead to subchondral bone sclerosis [27,28].

Mitophagy is a key process in the cell fate cycle that contributes to the removal of damaged and senescent mitochondria, thereby ensuring mitochondrial homeostasis and cell viability [29,30]. Mitochondria serve as the principal intracellular origin of reactive oxygen species (ROS) and stand as primary sites vulnerable to oxidative impairment. Additionally, these organelles play a central role in iron metabolism, overseeing the regulation and equilibrium of iron within the body [31,32]. Under physiological circumstances, mitophagy, fusion, and fission mechanisms operate individually or simultaneously to uphold a meticulous balance in mitochondrial quality control, thus ensuring an optimal functional state of these organelles [33]. Upon inhibition of mitophagy, the timely elimination of damaged mitochondria is impeded, fostering the accumulation of aggregated dysfunctional mitochondria, thereby culminating in mitochondrial dysfunction [34]. Studies have shown that in osteoarthritis, cartilage degeneration is closely associated with mitochondrial dysfunction as OA progresses, regulated and controlled by complex mechanisms [35,36].

Ferroptosis is a form of programmed cell death caused by iron-dependent lipid peroxidation [8], its main features are: depletion of glutathione, accumulation of ferrous ions and production of lipid peroxides [37]. Recent studies suggest that chondrocyte ferroptosis plays a key role in the development of OA [38,39]. Moreover, a myriad of connections has been delineated between ferroptosis and mitochondrial dysfunction. Ferroptosis coincides with heightened reactive oxygen species (ROS) generation, while the perturbation of ATP synthesis

results in irregular iron transportation pathways [40–42]. Multiple investigations have elucidated the correlation between ferroptosis and the process of mitophagy. For instance, Bi et al. highlighted the interaction between Fundc1 and Gpx4, showcasing their role in promoting hepatic ferroptosis and fibrotic injury via mitophagy-dependent pathways [43]. Similarly, Lin et al. discovered that BNIP3 and the PINK1-PARK2 pathway regulate mitophagy, shielding renal tubular epithelial cells against cisplatin-induced fibrosis via the ROS/HO1/Gpx4 axis [44]. However, the potential interaction between mitophagy and ferroptosis during osteoarthritis development remains unclear. Therefore, we experimentally elucidated the level of mitophagy that regulates ferroptosis. However, it was previously reported in the literature that ROS cause depolarization of the mitochondrial membrane potential and induce an increase in mitophagy, which seems to be contradictory to the preliminaries results like [18]. During the initial stages of osteoarthritis (OA), the accrual of reactive oxygen species (ROS) triggers the spontaneous activation of mitophagy, constituting an active defense mechanism. However, in the advanced phases of OA, the depletion of Parkin results in dysfunctional mitophagy [20].

The current study still has some limitations. First, regarding the relationship between mitophagy and ferroptosis, it may be limited to verify the correlation only from proteins, and it may be possible to reveal the relationship at the level of the single-cell transcriptome. Second, our study demonstrated that JP4-039 significantly inhibited chondrocyte ferroptosis by promoting Pink1/Parkin-dependent mitophagy, thereby slowing the progression of osteoarthritis. However, the possibility of potential mechanisms of mitophagy by other pathways cannot be ignored. In addition, we explored the existence of a negative correlation between mitophagy and ferroptosis in six clinical samples. Small sample sizes may compromise current studies of clinical specimens, leading to potential selection bias and other implications. Therefore, further prospective studies or the use of larger cohorts to confirm our findings are imperative.

5. Conclusions

In this study, we confirmed the correlation between mitophagy and ferroptosis. This work demonstrated that JP4-039 promotes mitophagy to inhibit ferroptosis in chondrocytes, proving its potential as a therapeutic agent for osteoarthritis.

Authors' contributions

All authors have critically reviewed and approved the final manuscript to be published. YX, ZL and WL took responsibility for the integrity of the data and the accuracy of the data analysis. Study conception and design: DS, YX and ZL. Acquisition of data: WL, JL, WS, HG and XJ. Analysis and interpretation of data: YL, JR, YF, and RW. Authorship note: YX, ZL and WL contributed equally to this work.

Ethics approval and consent to participate

The study was conducted in accordance with the Declaration of Helsinki, and approved by the Ethical Committee of the Nanjing Drum Tower Hospital, Affiliated Hospital of Medical School, Nanjing University (2009022). The animal study protocol was approved by the Animal Care and Use Committee of Nanjing Drum Tower Hospital, Affiliated Hospital of Medical School, Nanjing University (2020AE01102).

Funding

This work was supported by National Science Foundation of China (82325035, 82172481, 32271409), Six Talent Peaks Project of Jiangsu Province (WSW-079),Innovation Project of National Orthopedics and Sports Medicine Rehabilitation Clinical Medical Research Center (2021-NCRC-CXJJ-ZH-16).

Conflicts of interest

The authors declare that they have no competing interests.

6. Acknowledgements

Not applicable.

Appendix A. Supplementary data

Supplementary data to this article can be found online at https://doi.org/10.1016/j.jot.2025.01.001.

References

[1] Hunter DJ, March L, Chew M. Osteoarthritis in 2020 and beyond: a lancet commission. Lancet 2020;396(10264):1711–2 [eng].
[2] Hunter DJ, Bierma-Zeinstra S. Osteoarthritis. Lancet 2019;393(10182):1745–59 [eng].
[3] Hunter DJ, Schofield D, Callander E. The individual and socioeconomic impact of osteoarthritis. Nat Rev Rheumatol 2014;10(7):437–41 [eng].
[4] Latourte A, Kloppenburg M, Richette P. Emerging pharmaceutical therapies for osteoarthritis. Nat Rev Rheumatol 2020;16(12):673–88 [eng].
[5] Lv Z, Yang YX, Li J, Fei Y, Guo H, Sun Z, et al. Molecular classification of knee osteoarthritis. Front Cell Dev Biol 2021;9:725568 [eng].
[6] An S, Hu H, Li Y, Hu Y. Pyroptosis plays a role in osteoarthritis. Aging and disease 2020;11(5):1146–57 [eng].
[7] Charlier E, Relic B, Deroyer C, Malaise O, Neuville S, Collée J, et al. Insights on molecular mechanisms of chondrocytes death in osteoarthritis. Int J Mol Sci 2016;17(12) [eng].
[8] Dixon SJ, Lemberg KM, Lamprecht MR, Skouta R, Zaitsev EM, Gleason CE, et al. Ferroptosis: an iron-dependent form of nonapoptotic cell death. Cell 2012;149(5):1060–72 [eng].
[9] Chehade S, Adams PC. Severe hemochromatosis arthropathy in the absence of iron overload. Hepatology 2019;70(3):1064–5 [eng].
[10] Yao X, Sun K, Yu S, Luo J, Guo J, Lin J, et al. Chondrocyte ferroptosis contribute to the progression of osteoarthritis. J Orthop Translat 2021;27:33–43 [eng].
[11] Lv Z, Han J, Li J, Guo H, Fei Y, Sun Z, et al. Single cell RNA-seq analysis identifies ferroptotic chondrocyte cluster and reveals TRPV1 as an anti-ferroptotic target in osteoarthritis. EBioMedicine 2022;84:104258 [eng].
[12] Luo J, Mills K, le Cessie S, Noordam R, van Heemst D. Ageing, age-related diseases and oxidative stress: what to do next? Ageing Res Rev 2020;57:100982 [eng].
[13] Yousefzadeh M, Henpita C, Vyas R, Soto-Palma C, Robbins P, Niedernhofer L. DNA damage-how and why we age? Elife 2021;10 [eng].
[14] Paul BT, Manz DH, Torti FM, Torti SV. Mitochondria and Iron: current questions. Expert review of hematology 2017;10(1):65–79 [eng].
[15] Yagoda N, von Rechenberg M, Zaganjor E, Bauer AJ, Yang WS, Fridman DJ, et al. RAS-RAF-MEK-dependent oxidative cell death involving voltage-dependent anion channels. Nature 2007;447(7146):864–8 [eng].
[16] Yang WS, Stockwell BR. Synthetic lethal screening identifies compounds activating iron-dependent, nonapoptotic cell death in oncogenic-RAS-harboring cancer cells. Chemistry & biology 2008;15(3):234–45 [eng].
[17] Gao M, Yi J, Zhu J, Minikes AM, Monian P, Thompson CB, et al. Role of mitochondria in ferroptosis. Molecular cell 2019;73(2). 354-63.e3. [eng].
[18] Lu Y, Li Z, Zhang S, Zhang T, Liu Y, Zhang L. Cellular mitophagy: mechanism, roles in diseases and small molecule pharmacological regulation. Theranostics 2023;13(2):736–66 [eng].
[19] Sun K, Jing X, Guo J, Yao X, Guo F. Mitophagy in degenerative joint diseases. Autophagy 2021;17(9):2082–92 [eng].
[20] Ansari MY, Khan NM, Ahmad I, Haqqi TM. Parkin clearance of dysfunctional mitochondria regulates ROS levels and increases survival of human chondrocytes. Osteoarthritis Cartilage 2018;26(8):1087–97 [eng].
[21] Chu C, Wang X, Yang C, Chen F, Shi L, Xu W, et al. Neutrophil extracellular traps drive intestinal microvascular endothelial ferroptosis by impairing Fundc1-dependent mitophagy. Redox Biol 2023;67:102906 [eng].
[22] Krainz T, Gaschler MM, Lim C, Sacher JR, Stockwell BR, Wipf P. A mitochondrial-targeted nitroxide is a potent inhibitor of ferroptosis. ACS Cent Sci 2016;2(9):653–9 [eng].
[23] Glänzel NM, Grings M, da Rosa-Junior NT, de Carvalho LMC, Mohsen AW, Wipf P, et al. The mitochondrial-targeted reactive species scavenger JP4-039 prevents sulfite-induced alterations in antioxidant defenses, energy transfer, and cell death signaling in striatum of rats. J Inherit Metab Dis 2021;44(2):481–91 [eng].
[24] Zhu X, Chen F, Lu K, Wei A, Jiang Q, Cao W. PPARγ preservation via promoter demethylation alleviates osteoarthritis in mice. Annals of the rheumatic diseases 2019;78(10):1420–9 [eng].
[25] Allen J, Imbert I, Havelin J, Henderson T, Stevenson G, Liaw L, et al. Effects of treadmill exercise on advanced osteoarthritis pain in rats. Arthritis Rheumatol 2017;69(7):1407–17 [eng].
[26] Carlson EL, Karuppagounder V, Pinamont WJ, Yoshioka NK, Ahmad A, Schott EM, et al. Paroxetine-mediated GRK2 inhibition is a disease-modifying treatment for osteoarthritis. Sci Transl Med 2021;13(580) [eng].

[27] Lajeunesse D, Reboul P. Subchondral bone in osteoarthritis: a biologic link with articular cartilage leading to abnormal remodeling. Curr Opin Rheumatol 2003;15(5):628–33 [eng].
[28] Ni Z, Zhou S, Li S, Kuang L, Chen H, Luo X, et al. Exosomes: roles and therapeutic potential in osteoarthritis. Bone Res 2020;8:25 [eng].
[29] Eldeeb MA, Thomas RA, Ragheb MA, Fallahi A, Fon EA. Mitochondrial quality control in health and in Parkinson's disease. Physiol Rev 2022;102(4):1721–55 [eng].
[30] Zhang C, Gao X, Li M, Yu X, Huang F, Wang Y, et al. The role of mitochondrial quality surveillance in skin aging: focus on mitochondrial dynamics, biogenesis and mitophagy. Ageing Res Rev 2023;87:101917 [eng].
[31] Jain IH, Calvo SE, Markhard AL, Skinner OS, To TL, Ast T, et al. Genetic screen for cell fitness in high or low oxygen highlights mitochondrial and lipid metabolism. Cell 2020;181(3). 716-27.e11. [eng].
[32] Read AD, Bentley RE, Archer SL, Dunham-Snary KJ. Mitochondrial iron-sulfur clusters: structure, function, and an emerging role in vascular biology. Redox Biol 2021;47:102164 [eng].
[33] Song J, Herrmann JM, Becker T. Quality control of the mitochondrial proteome. Nat Rev Mol Cell Biol 2021;22(1):54–70 [eng].
[34] Bock FJ, Tait SWG. Mitochondria as multifaceted regulators of cell death. Nat Rev Mol Cell Biol 2020;21(2):85–100 [eng].
[35] Fang G, Wen X, Jiang Z, Du X, Liu R, Zhang C, et al. FUNDC1/PFKP-mediated mitophagy induced by KD025 ameliorates cartilage degeneration in osteoarthritis. Mol Ther : the journal of the American Society of Gene Therapy 2023;31(12):3594–612 [eng].
[36] Liu L, Zhang W, Liu T, Tan Y, Chen C, Zhao J, et al. The physiological metabolite α-ketoglutarate ameliorates osteoarthritis by regulating mitophagy and oxidative stress. Redox Biol 2023;62:102663 [eng].
[37] Jiang X, Stockwell BR, Conrad M. Ferroptosis: mechanisms, biology and role in disease. Nat Rev Mol Cell Biol 2021;22(4):266–82 [eng].
[38] Miao Y, Chen Y, Xue F, Liu K, Zhu B, Gao J, et al. Contribution of ferroptosis and GPX4's dual functions to osteoarthritis progression. EBioMedicine 2022;76:103847 [eng].
[39] Wang S, Li W, Zhang P, Wang Z, Ma X, Liu C, et al. Mechanical overloading induces GPX4-regulated chondrocyte ferroptosis in osteoarthritis via Piezo1 channel facilitated calcium influx. J Adv Res 2022;41:63–75 [eng].
[40] Liu C, Li Z, Li B, Liu W, Zhang S, Qiu K, et al. Relationship between ferroptosis and mitophagy in cardiac ischemia reperfusion injury: a mini-review. PeerJ 2023;11:e14952 [eng].
[41] Granata S, Votrico V, Spadaccino F, Catalano V, Netti GS, Ranieri E, et al. Oxidative stress and ischemia/reperfusion injury in kidney transplantation: focus on ferroptosis. Mitophagy and New Antioxidants. Antioxidants (Basel, Switzerland) 2022;11(4) [eng].
[42] Li W, Xiang Z, Xing Y, Li S, Shi S. Mitochondria bridge HIF signaling and ferroptosis blockage in acute kidney injury. Cell Death Dis 2022;13(4):308 [eng].
[43] Bi Y, Liu S, Qin X, Abudureyimu M, Wang L, Zou R, et al. FUNDC1 interacts with GPx4 to govern hepatic ferroptosis and fibrotic injury through a mitophagy-dependent manner. J Adv Res 2023 [eng].
[44] Lin Q, Li S, Jin H, Cai H, Zhu X, Yang Y, et al. Mitophagy alleviates cisplatin-induced renal tubular epithelial cell ferroptosis through ROS/HO-1/GPX4 axis. Int J Biol Sci 2023;19(4):1192–210 [eng].